energies

MDPI

Article

Research on Distribution Network Fault Location Based on Electric Field Coupling Voltage Sensing and Multi-Source Information Fusion

Bo Li [1], Lijun Tang [1], Zhiming Gu [1], Li Liu [2,*] and Zhensheng Wu [2]

[1] Yunnan Power Grid Co., Ltd., Electric Power Science Research Institute, Kunming 650217, China; jlsgaoya307@163.com (B.L.); tlijun@foxmail.com (L.T.); dkygzm@163.com (Z.G.)
[2] School of Electrical Engineering, Beijing Jiaotong University, Beijing 100044, China; zhshwu@bjtu.edu.cn
* Correspondence: 23126318@bjtu.edu.cn

Abstract: As the last link of power transmission, the safe operation of the distribution network directly affects the experience of power users, and short-time distribution network faults can cause huge economic losses. There are few fault recording devices in rural or suburban distribution networks, and it is difficult to upload information, which brings difficulties to accurate fault location. In order to improve the accuracy of fault location, this study proposes a fault location method for distribution networks based on electric field-coupled voltage sensing and multi-source information fusion. First, an optimized resource pool architecture is proposed, and a distribution network data fusion platform is established based on this architecture to effectively integrate voltage, current and other fault data. Second, in order to overcome the problem of expanding the fault location range that may be caused by the current-based matrix algorithm, this study proposes an improved directed graph-based matrix algorithm and combines it with the matrix algorithm of voltage quantities to form a joint location criterion, which improves the accuracy of fault location. Finally, for the single-ended ranging method, which is easily affected by the wave impedance discontinuity points in the system or the transition resistance in the line, this article introduces a fault ranging algorithm based on double-ended electrical quantities, which improves the accuracy and applicable range of fault ranging. Through simulation verification, we found that the matrix algorithm based on the electrical quantity can accurately locate the fault section in the case of a single fault with a single power supply. The proposed joint matrix algorithm can accurately locate the fault section in the case of a single fault with multiple power sources. The ranging algorithm based on double-ended electrical quantities has higher ranging accuracy in both interphase short circuits and grounded short circuits, and the ranging results are not affected by the fault type, fault location and transition resistance, which can effectively improve the efficiency and reliability of fault location.

Keywords: fault location; fault ranging; matrix algorithm; double-end ranging; data fusion

check for updates

Academic Editor: Hugo Morais

Received: 30 December 2024
Revised: 8 February 2025
Accepted: 10 February 2025
Published: 13 February 2025

Citation: Li, B.; Tang, L.; Gu, Z.; Liu, L.; Wu, Z. Research on Distribution Network Fault Location Based on Electric Field Coupling Voltage Sensing and Multi-Source Information Fusion. *Energies* **2025**, *18*, 913. https://doi.org/10.3390/en18040913

Copyright: © 2025 by the authors. Licensee MDPI, Basel, Switzerland. This article is an open access article distributed under the terms and conditions of the Creative Commons Attribution (CC BY) license (https://creativecommons.org/licenses/by/4.0/).

1. Introduction

Fault detection in distribution networks is a crucial component of distribution network automation, with the fault location being fundamental to this detection process. Research shows that 95% of power outage accidents in distribution networks are caused by abnormal operating conditions, and most of them are caused by distribution network faults [1]. For rural or suburban power grids, the relatively low automation level and long distribution

lines with large coverage areas bring many difficulties to accurate fault location. In addition, the structure of the distribution network is becoming increasingly complex, and the traditional fault location methods struggle to accurately determine the fault section, especially as in a multi-power supply system, the fault current may flow to the fault point from multiple directions, which leads to the expansion of the positioning range of the matrix algorithm based on current, and through the introduction of matrix algorithms based on voltage, the significance of the voltage change can be used to further confirm the fault section and reduce the misjudgment. In recent years, the automation level of distribution networks has been gradually improved, and it is no longer difficult to obtain multi-source data from different systems and terminals. If these multi-source fault data can be fully utilized, combined with the improved matrix algorithm, the accuracy of fault location can be improved to a certain extent, and the reliability of the power supply in distribution networks can be improved, and the economic losses due to faults can be reduced.

According to the different location results, distribution network fault location is mainly divided into three types: fault line selection, fault section location and fault ranging [2]. The method of fault section location in a distribution network mainly includes a direct algorithm represented by a matrix method and an indirect algorithm represented by an artificial intelligence algorithm. The traditional matrix method has a low fault tolerance rate and a high dependence on data. The complex structure of the distribution network and the access to a distributed power supply all reduce the accuracy of fault location. In view of this, many scholars have made many improvements to the matrix method. Reference [3] proposed the concept of a network relationship moment. According to the topological structure of the network, the network relationship moment is constructed, so that the rows and columns of the matrix represent the dependence between nodes and the theoretical state of nodes when the equipment fails. The matrix represents more abundant information, the operation does not need to be standardized and the proportion of computing resources is small. In reference [4], the fault distance matrix was established by using the traveling wave information obtained using high-frequency sampling between the main line and the branch line of the distribution network, and the error matrix was generated by reducing the dimension of the fault distance matrix according to the actual situation of the field, which could effectively reduce the number of detection devices and improve the accuracy of detection. The access to distributed power makes the traditional matrix algorithm no longer applicable. Reference [5] proposed an improved matrix algorithm based on the positive direction of the switching power flow. It only needs to determine the positive direction of the power flow once for different power supplies to generate a new fault discrimination matrix, which can effectively improve the operation speed. Reference [6] constructed a directional network topology matrix by using the installation position of the fault indicator (FI) and set the delay parameter T considering the communication delay problem to collect the fault information. This method effectively avoids the problem of a terminal blind area and improves the integrity of fault information. In reference [7], for a neutral point grounding system using an arc suppression coil, the fault information matrix was formed by judging the change in the zero-sequence current after conversion, and a unified criterion was proposed. This method has good fault tolerance, adaptability and real-time performance in different situations such as multiple feeder faults. In reference [8], concerning the large number of calculations in the normalized processing of fault determination using the traditional matrix algorithm, a fault location method for distribution networks based on an improved matrix algorithm was proposed. This method can accurately identify the fault area according to the collected fault information component and can locate the fault area quickly and effectively. Reference [9] proposed an improved section location algorithm based on the matrix algorithm. Using the structure description matrix and fault information

matrix to obtain the fault judgment matrix, according to their different composition, the row elements in the matrix corresponding to the section were divided into types of zones, with the establishment of each type of section under the fault criterion reflecting all the faults, and then the section where the fault occurred was determined. Reference [10] proposed a fault location matrix algorithm based on voltage magnitude correction for distribution networks, and the effectiveness of the method was verified through simulation and actual testing, which effectively solved the problem of the traditional fault location algorithm not being accurate enough to locate faults on "T"-shaped lines. Compared with the matrix method based on the network topology, the artificial intelligence method based on data training has a higher fault tolerance rate. When the data are distorted and mistakenly transmitted, the robustness is good, so it can effectively target a distribution network system with weak fault characteristics and a complex network structure. Reference [11] proposes a location method based on deep learning. It was proved that the algorithm can extract fault features automatically and is not affected by the fault type and fault time. In reference [12], considering the large amount of access to distributed power sources, adaptive genetic particle swarm optimization was selected for fault location. In reference [13], the graph theory method was combined with an artificial intelligence algorithm, and the information uploaded by the distribution network detection unit was used to generate the adjacency matrix, and the connectivity equivalent model of the fault current in the topology was established. In the aspect of the fault information processing of distribution networks, reference [14] pointed out that a synchronous phasor measurement unit can be used to provide support. The real-time updating of section information was realized using an adjacent sub-array method. The short circuit fault section location algorithm was adopted, and the algorithm was verified through simulation. The results showed that the algorithm has the ability to deal with the information change caused by the change in the topology.

Fault ranging is the final link of fault location technology, which is the most difficult. According to the different information used for fault location, fault location can be divided into the injection method [15], impedance analysis method [16], traveling wave ranging method [17] and an artificial intelligence algorithm. Gernot Druml proposed a new fast pulse detection method for high-power current injection and carried out actual field tests. It was proved that this method can reduce the harmonic effect in the fault current and reduce the requirement for the angle accuracy of the current transformer [18]. Reference [19] used wavelet pulses to realize ranging after local maximum detection, and the ranging accuracy and anti-noise interference ability were improved to a certain extent. The impedance analysis method is mainly divided into single-ended and double-ended ranging. In recent years, research has focused on double-ended ranging. Reference [20] determined the system impedance and line parameters using the longitudinal impedance of the line and then adjusted the calculated line parameters by incorporating the fault distance obtained from the lumped parameter model. References [21,22] reduced the influence of asynchronous angle and line parameters, which had certain advantages compared with several commonly used two-terminal asynchronous algorithms. In reference [23], a ranging method based on parameter identification was proposed. Reference [24] used the least square method and line parameters to realize the synchronization of the recorded data at both ends. The key to traveling wave ranging is the synchronization of time and the capture of the traveling wave head. There are also studies on the correction of the wave velocity [25–27]. In reference [28], taking into account the time delay caused by the time-varying effect of the line fault on the traveling wave transmission, a ranging algorithm for compensating for the time delay of the distribution transformer was proposed. Reference [29] proposed a distribution network fault location method based on the multi-terminal traveling wave time difference. According to the three-terminal traveling wave method, the actual fault distance was

calculated to eliminate the ranging error caused by the uncertainty of the traveling wave velocity. Reference [30] used a continuous wavelet transform applied to a series of line current measurements obtained from a distributed network of optical sensors, taking into account the different fault resistances, mother wavelets, scaling factors and noise inputs. With the development of computer technology, artificial intelligence algorithms are widely used in fault location for distribution networks, such as the ant colony algorithm, neural network algorithm and so on. References [31,32] have constructed an optimization model of fault location based on the ant colony algorithm. Reference [33] introduced an adaptive elite strategy and adaptive mutation operation into the multiverse algorithm and designed an update mechanism to improve the local optimization and global optimization ability of the algorithm, but it lacked comparison with the algorithm before improvement, and the positioning accuracy needs to be improved. Although artificial intelligence algorithms have a high ranging accuracy and strong applicability, they do not need to consider the influence of the fault type, transition resistance, non-synchronous angle, etc., but they require a large number of fault data training models, and the acquisition and processing of fault samples are difficult.

From the above research, it can be seen that most of the current literature does not fully consider the importance of the real-time collection and uploading of fault data in rural or suburban power grids, and the artificial intelligence method is complex in the network. When the computing resources increase, the data processing speed decreases, and the time required for fault location will increase. In addition, in some studies, the single-ended ranging method was easily affected by the wave impedance discontinuity point in the system or the transition resistance in the line. In view of the above problems, this study proposes a fault location algorithm based on double-ended electrical quantities, which makes full use of double-ended electrical information to reduce the influence of transition resistance in the single-ended fault location method. The main contributions of this study are as follows:

(1) Starting from the data source of distribution network fault location, it is explained that the data sources for fault location are the terminal unit, GIS system, IoT terminal measurement device and other data. The resource pool is optimized into a 'three-layer two-line' structure, and a distribution network data fusion platform based on the resource pool is established for power grid data fusion, which ensures the rational and full utilization of heterogeneous and multi-source fault information.

(2) Considering that the error in the single-ended ranging method is related to the line structure or fault state, which is difficult to avoid, this study proposes a fault ranging algorithm based on double-ended electrical quantities, which makes full use of the double-ended electrical information to reduce the influence of the transition resistance in the single-ended ranging method. Through simulation analysis, the ranging results were compared with those of the single-ended ranging algorithm to verify the effectiveness of the proposed model.

In this study, the heterogeneous data from different terminals and different systems are fused through the distribution network data fusion platform based on the resource pool, which ensures the full utilization of multi-source fault information. In addition, we improve the directed graph-based matrix algorithm and propose a joint matrix algorithm for fault section location for multi-supply power systems. After selecting the correct fault section, a fault ranging algorithm based on double-ended electrical quantities is proposed, and the effectiveness of the double-ended ranging algorithm is verified. This study addresses the limitation of traditional fault location using a single electrical quantity, which is easily affected by wave impedance discontinuities in the system or transition resistances in the line. Through these innovations, this algorithm provides more accurate fault location in the

complex structure of the distribution network, which is of great significance to improve the quality of the power supply in the distribution network and maintain a good and safe operating environment.

2. Fault Location Based on Multi-Source Data

With the development of the national economy, the scale and complexity of the power system are increasing. The traditional voltage sensing method has a large volume, high maintenance cost and poor flexibility for arrangement and movement, which cannot meet the needs of large-scale sensing. Based on the above problems, this article first introduces electric field coupling voltage sensing. The non-contact measurement technology does not need to invade the insulation layer of the wire or the inside of the power equipment, and it is also conducive to the safe and stable operation of the power grid while accurately measuring the voltage.

The key point of electric field coupling voltage sensing is to model the electrostatic field of the live conductor and to invert the power line voltage based on the inverse problem of the electric field. The calculation method of an electrostatic field can be used to calculate the electric field of a three-phase power line. Based on the equivalent charge method, it can be shown that the electric field in the region of the charged conductor is proportional to its potential. For any distribution line, whose boundary conditions are shown in Equation (1), the electric field near the line and its potential have a relationship as shown in Equation (2).

$$\begin{cases} \varphi_{R \le r_0} = \varphi(t) \\ \varphi_{R \to \infty} = 0 \end{cases} \tag{1}$$

$$\vec{E}(t) = \frac{r_0}{{R_0}^2} \varphi(t) \cdot \vec{e}_R \tag{2}$$

where $\vec{E}(t)$ is the electric field strength of the measuring point, R_0 is the distance between the measuring point and the center of the wire, r_0 is the half-diameter of the wire and $\varphi(t)$ is the potential of the measured wire.

When the sensor is in a space with an electric field intensity of $E(r,t)$, an induced charge will be generated on the surface of the metal electrode due to electrostatic induction, and the amount of charge is q. According to the Gauss theorem,

$$q = \oint_A \varepsilon_0 E(r,t) dA \tag{3}$$

When the electric field intensity changes with time, both sides of Equation (3) are differentiated at the same time, so then

$$\frac{dq}{dt} = \oint_A \varepsilon_0 \frac{dE(r,t)}{dt} dA \tag{4}$$

The voltage drop $V_0(t)$ on the load resistance R_m is caused by the current generated by the changing charge, and the relationship between them can be expressed as

$$V_0(t) = R_m \oint_A \varepsilon_0 \frac{dE(r,t)}{dt} dA \tag{5}$$

Substituting Equation (2) into Equation (5), the relationship between the measured conductor potential and the output of the sensor is as follows:

$$V_0(t) = R_m \frac{d\varphi(t)}{dt} \oint_A \varepsilon_0 \frac{r_0}{{R_0}^2} dA \tag{6}$$

The linear proportional coefficient between the measured conductor voltage $\varphi(t)$ and the sensor output signal $V_0(t)$ is defined as the sensor equivalent area A_{eq}:

$$A_{eq} = \oint_A \varepsilon_0 \frac{r^0}{{R_0}^2} dA \tag{7}$$

Finally, the relation between the output voltage $V_0(t)$ of the sensor and the potential of the measured conductor $\varphi(t)$ can be obtained as follows:

$$V_0(t) = R_m A_{eq} \frac{d\varphi(t)}{dt} \tag{8}$$

Therefore, it is only necessary to integrate the output measurement signal of the sensor in the time domain to obtain a measurement value that is linear with the conductor potential. Based on non-contact voltage measurement, the fault location method for distribution networks is studied in this article.

Fault location for distribution networks is a complex task, which cannot be completed by relying on a single data source. Data from different sources contain different fault information [34]. Therefore, the use of multi-source data for fault location research is necessary to improve the quality of the power supply distribution network.

Fault section location and fault location are two main aspects of accurate fault location in distribution networks. Fault section location mainly uses the terminal unit data of the distribution network and the GIS data for network topology analysis. Fault location is based on the fault recording data of the distribution network IoT terminal. Terminal unit data in this study refer to the feeder terminal unit, FTU, data. GIS system data can be obtained in the GIS, geographic information system. Fault recording data are the fault information collected by fault recording equipment. The terminal unit data of the Internet of Things are obtained by the terminal unit of the Internet of Things, which collects all electrical indicators at any time and any place on the distribution network and uploads them to the cloud [35].

In order to realize the unified management and scheduling of various systems and terminal resources in the distribution network, this article proposes a distribution network data fusion platform based on the resource pool, which integrates multi-source heterogeneous data from different systems and different devices. In the integrated scheduling data platform, the corresponding data are extracted or prioritized according to the business requirements.

Although the traditional resource pool architecture clearly defines the functional partition of the resource pool, which improves the efficiency of each layer's independent work, the overall structure is too complex, and when the Internet of Things terminal units are connected too much, the data to be processed by the resource pool will also surge. Therefore, this article proposes another optimized resource pool architecture. Based on the unified resource model, the architecture develops middleware tool set and provides a unified resource access interface for terminal resource registration. The following figure, Figure 1, shows the structure of the resource pool, which can be summarized as a three-layer and two-line structure.

The three-layer structure refers to the cooperative terminal layer, unified computing resource pool layer and resource management platform layer. Data are divided into two types, data flow and function flow, for efficient transmission and management. A unified computing resource pool handles both types of flows.

(1) Data flow: The resource pool continuously processes sensor fusion data uploaded by collaborative terminals, stores the data and allows for access to the stored information through the resource management platform to monitor the status and parameters.

(2) Function flow: This involves calling the controllable functions of the terminal access and verifying that the terminal is online to enable control. The platform's interface program is used to configure parameters and manage the devices of the connected terminals.

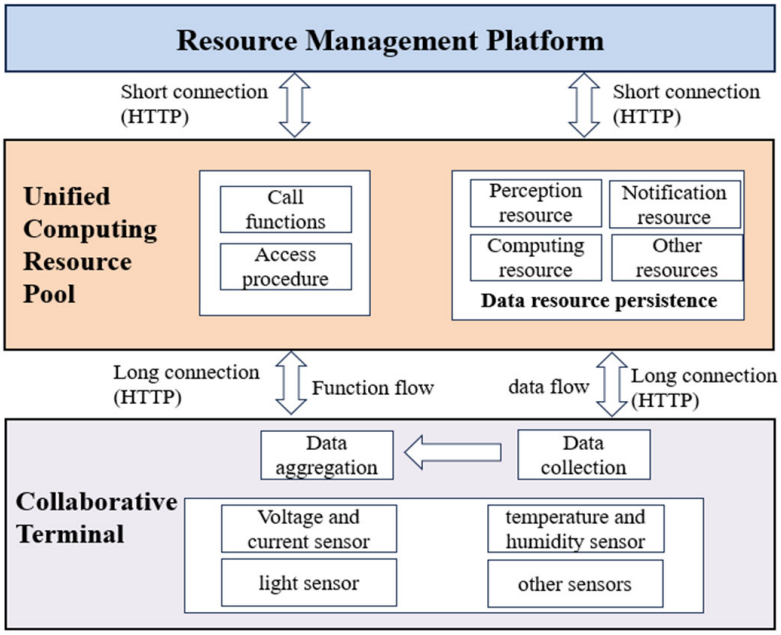


Figure 1. Optimized resource pool model.

The resource pool addresses the challenge of collaboration among diverse terminals, enhances the capacity for acquiring and consolidating data from multiple sources and bolsters the diagnostic capabilities for power system faults. The cloud computing resource pool framework outlined in this article is primarily constituted by a middleware toolkit, an application platform, a centralized computing resource pool and a resource management platform. It interfaces with terminal devices to facilitate the integrated processing of power data uploaded by these devices. The basic design process is shown in Figure 2:

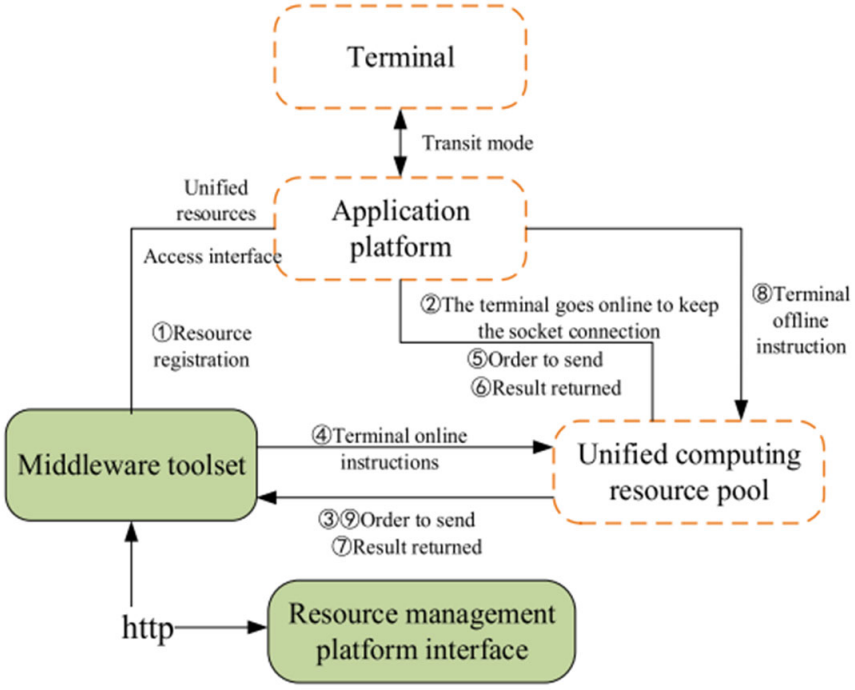


Figure 2. Resource pool data processing flow.

3. Distribution Network Fault Location Matrix Algorithm Based on Multiple Capacities

3.1. Distribution Network Topology Analysis Graph Theory Description

The distribution network has a relatively intricate network structure. In topology analysis, the less important research objects can be ignored to obtain a topology diagram that clearly describes the network relationship, and the distribution network can be analyzed more directly. According to reference [27], graphs can be represented as directed graphs and undirected graphs. The directed topology of a simple distribution network is shown in Figure 3.

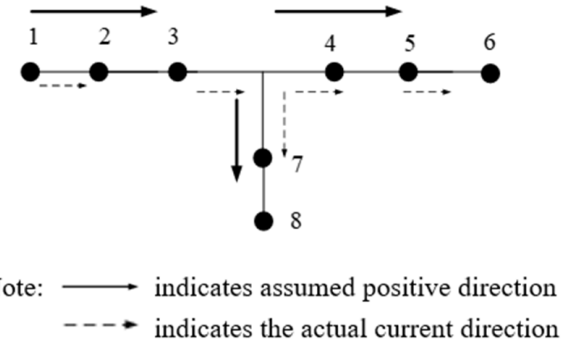


Figure 3. Simple distribution network with directional topology.

The bus entry switch and segment switch, feeder circuit breaker and segment switch, contact switch, etc., are regarded as a network node, and N nodes are obtained by numbering them. According to these N nodes, a square matrix can be constructed and represented by D, where D_{ij} indicates the connection relationship between nodes.

$$D = \begin{bmatrix} D_{11} & D_{12} & D_{13} & \cdots & D_{1n} \\ D_{21} & D_{22} & D_{23} & \cdots & D_{2n} \\ D_{31} & D_{32} & D_{33} & \cdots & D_{3n} \\ \cdots & \cdots & \cdots & \cdots & \cdots \\ D_{n1} & D_{n2} & D_{n3} & \cdots & D_{nn} \end{bmatrix} \tag{9}$$

When a directed graph is used to describe the structure of the distribution network, the direction of the line's current is specified as the positive direction of the feeder. The D element of the matrix is set as follows:

$$D_{ij} = \begin{cases} i \neq j, \begin{cases} 0, \textit{Indicates that nodes i and j are not connected} \\ 1, \textit{Indicates that a positive current exists on the feeder line between nodes i and j} \end{cases} \\ i = j, 0 \end{cases} \tag{10}$$

Thus, the network description matrix D of the distribution network shown in Figure 3 can be obtained as follows:

$$D = \begin{bmatrix} 0 & 1 & 0 & 0 & 0 & 0 & 0 & 0 \\ 0 & 0 & 1 & 0 & 0 & 0 & 0 & 0 \\ 0 & 0 & 0 & 1 & 0 & 0 & 1 & 0 \\ 0 & 0 & 0 & 0 & 1 & 0 & 0 & 0 \\ 0 & 0 & 0 & 0 & 0 & 1 & 0 & 0 \\ 0 & 0 & 0 & 0 & 0 & 0 & 0 & 0 \\ 0 & 0 & 0 & 0 & 0 & 0 & 0 & 1 \\ 0 & 0 & 0 & 0 & 0 & 0 & 0 & 0 \end{bmatrix} \tag{11}$$

When using the matrix algorithm based on a directed topology graph for fault localization, firstly, the directed network description matrix D is generated according to Equation (10); secondly, when a fault occurs in the distribution network, the fault information matrix P is generated based on the overcurrent information transmitted to the system; and lastly, the fault location is determined in accordance with the specified fault discrimination conditions. The algorithm does not require specification processing, the amount of arithmetic is greatly reduced, the fault criterion is relatively simple and theoretically there is no misjudgment.

3.2. Improved Matrix Algorithm Based on Directed Graph

Conventional fault location methods treat contact switches and circuit breakers within the network as nodes. Given the complexity of modern distribution network structures and the increasing number of switchgears, considering them all as nodes would prolong fault identification times [36–38]. This article simplifies the network topology by designating only the switchgear at the outgoing end of the bus as nodes in the network description matrix, significantly reducing the network node count and matrix size. At the same time, the power flow direction of the last moment in the distribution network is regarded as the prescribed positive direction, and an improved matrix algorithm based on a directed graph is proposed with good applicability.

3.2.1. Network Description Matrix

In Figure 4, for example, the measuring point where the terminal device is installed is regarded as a node. There are eight nodes in the figure; node 1 is a power point. The arrow of the solid black line indicates the real-time power flow direction in the system, which is taken as the positive direction of the network. The current direction may differ from this defined positive direction only in the event of a line fault. The network description matrix for the simple distribution network shown in Figure 4 can be derived from Equation (12):

$$D = \begin{bmatrix} 0 & 1 & 0 & 0 & 0 & 0 & 0 & 0 \\ 0 & 0 & 1 & 0 & 0 & 0 & 0 & 0 \\ 0 & 0 & 0 & 1 & 0 & 0 & 1 & 0 \\ 0 & 0 & 0 & 0 & 1 & 0 & 0 & 0 \\ 0 & 0 & 0 & 0 & 0 & 1 & 0 & 0 \\ 0 & 0 & 0 & 0 & 0 & 0 & 0 & 0 \\ 0 & 0 & 0 & 0 & 0 & 0 & 0 & 1 \\ 0 & 0 & 0 & 0 & 0 & 0 & 0 & 0 \end{bmatrix} \quad (12)$$

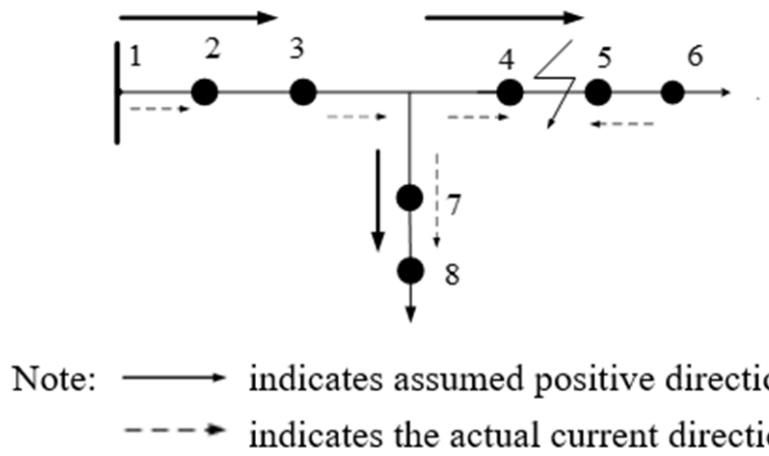


Figure 4. Distribution network simple fault diagram.

3.2.2. Fault Judgment Matrix

The fault discrimination matrix is a matrix of the order $N \times N$, which is obtained by modifying the diagonal elements of the network description matrix (the non-diagonal elements remain unchanged). The setting of diagonal elements is determined according to the fault information uploaded by the node. If a fault current flows through the node in a positive direction, the diagonal elements of the corresponding matrix are set to 1. If a fault current flows through the node in the opposite direction, the diagonal elements of the corresponding matrix are set to -1. If no fault current flows, the diagonal elements of the corresponding matrix are unchanged, that is, 0. The setting rules are as follows:

$$G_{ii} = \begin{cases} 1, \text{Node i has a fault current. The fault current is positive} \\ -1, \text{Node i has a fault current.The fault current is opposite} \\ 0, \text{No fault current flows through node i} \end{cases} \quad (13)$$

Assuming that there is a fault between nodes 4 and 5 in Figure 4, both nodes 3 and 4 can monitor the overcurrent. The fault discriminant matrix can be obtained by modifying the network description matrix:

$$P = \begin{bmatrix} 0 & 1 & 0 & 0 & 0 & 0 & 0 & 0 \\ 0 & 0 & 1 & 0 & 0 & 0 & 0 & 0 \\ 0 & 0 & 1 & 1 & 0 & 0 & 1 & 0 \\ 0 & 0 & 0 & 1 & 1 & 0 & 0 & 0 \\ 0 & 0 & 0 & 0 & 0 & 1 & 0 & 0 \\ 0 & 0 & 0 & 0 & 0 & 0 & 0 & 0 \\ 0 & 0 & 0 & 0 & 0 & 0 & 0 & 1 \\ 0 & 0 & 0 & 0 & 0 & 0 & 0 & 0 \end{bmatrix} \quad (14)$$

3.2.3. Failure Criterion

The setting principle of the fault criterion is that when a fault occurs in a certain area, the fault current at both ends of the fault flows to the fault point. From this, the following criterion can be obtained. When the elements in the fault discriminant matrix satisfy any of the following discriminant principles, the fault can be determined to occur in the corresponding interval:

(1) If $P_{ii} = 1$, and for all $i \neq j$, $P_{ij} = 0$, it can be considered that the fault occurs at the end of the feeder line after node i;
(2) If $P_{ii} = 1$, when $i \neq j$, for all $P_{ij} = 1$, $P_{jj} = -1$ or 0; it can be considered that the fault occurs between nodes i and j;
(3) If $P_{ii} = -1$, when $i \neq j$, $P_{ii} = 0$ for all $P_{ji} = 1$; it can be considered that the fault occurs between nodes i and j.

3.3. Fault Location Matrix Algorithm Based on Voltage Quantities

The traditional fault location matrix algorithm uses the fault current information provided by the FTU, but the simulation found that the upper level of the main line connected to the fault line can often collect the overcurrent information, and the end of the feeder connected to the main line will be considered as the fault node, resulting in the expansion of the fault location range [39]. When the power line fails, the voltage of the fault point will change greatly. Based on this, this section proposes a matrix algorithm based on the voltage quantity, which, together with the matrix algorithm based on the fault current, constitutes a joint fault location criterion.

3.3.1. Fault Judgment Matrix

The fault identification matrix based on the voltage is generated according to whether the node detects the fault voltage. China stipulates that for lines higher than 35 kV, the power supply voltage deviation value should be less than 10%. In the simulation process, it was found that the voltage of adjacent nodes will be reduced by at least 30% when a fault occurs. Therefore, this article identifies the nodes with a voltage reduction of more than 30% as voltage-abnormal nodes. The terminal equipment detects the fault information and uploads it to the main station system. The main station system selects the node with the most voltage reduction by comparing the voltage of the abnormal nodes, which is identified as the fault node, and corrects the diagonal elements in the network description matrix: if the node is a fault node, the corresponding matrix's diagonal element is set to 1; if the node is not the fault node, the corresponding matrix's diagonal element is set to 0. The setting principles are as follows:

$$P_{ii} = \begin{cases} 1, \text{The node is a faulty node.} \\ 0, \text{The node is not a faulty node.} \end{cases} \tag{15}$$

As shown in Figure 4, when a fault occurs between nodes 4 and 5, assuming that the voltage of nodes 4, 5 and 6 is abnormal and the voltage of node 5 decreases more, the fault discrimination matrix P can be obtained by modifying the D matrix as follows:

$$P = \begin{bmatrix} 0 & 1 & 0 & 0 & 0 & 0 & 0 & 0 \\ 0 & 0 & 1 & 0 & 0 & 0 & 0 & 0 \\ 0 & 0 & 0 & 1 & 0 & 0 & 0 & 0 \\ 0 & 0 & 0 & 0 & 1 & 0 & 0 & 0 \\ 0 & 0 & 0 & 0 & 1 & 1 & 0 & 0 \\ 0 & 0 & 0 & 0 & 0 & 0 & 0 & 0 \\ 0 & 0 & 0 & 0 & 0 & 0 & 0 & 1 \\ 0 & 0 & 0 & 0 & 0 & 0 & 0 & 0 \end{bmatrix} \tag{16}$$

3.3.2. Failure Criterion

The setting principle of the fault criterion is as follows: when a fault occurs in a certain section, the voltage at both ends of the fault point will greatly deviate from the normal value, and the node voltage will decrease the most in the whole power system, and the node voltage in the non-fault section will change relatively little. Therefore, when the elements in the fault discrimination matrix meet any of the following discrimination principles, the fault segment can be determined. If multiple criteria are met at the same time, multiple fault segments can be identified.

(1) If $P_{ii} = 1$, when $j \neq i$, $P_{ii} = 0$ for all $P_{ji} = 1$; it can be considered that the fault occurs between nodes i and j.
(2) If $P_{ii} = 1$ and for all $i \neq j$, $P_{ij} = 0$, it can be considered that the fault occurs at the end of the feeder line after the node.

3.4. Simulation Verification of Fault Section Location

Most of the distribution networks in China adopt a neutral point that is ungrounded or grounded by an arc suppression coil. Different grounding methods will cause different fault characteristics. For a system grounded by an arc suppression coil, the fault characteristics are obviously different when different compensation methods are adopted. If the system adopts the arc suppression coil grounding method, the appropriate arc suppression coil value must be selected.

As shown in Figure 5, the resistance value in the arc suppression coil is not counted in the analysis. It can be seen from Figure 5 that when the ground fault occurs, the ground current is $\dot{I}_L + \dot{I}_C$, where $\dot{I}_L$ is the inductance current flowing through the arc suppression coil, and $\dot{I}_C$ is the ground capacitance current. The ground capacitance current of the overhead line has the following two calculation methods:

(1) Using single-phase capacitance, $I_C = \sqrt{3} U_P \omega C$

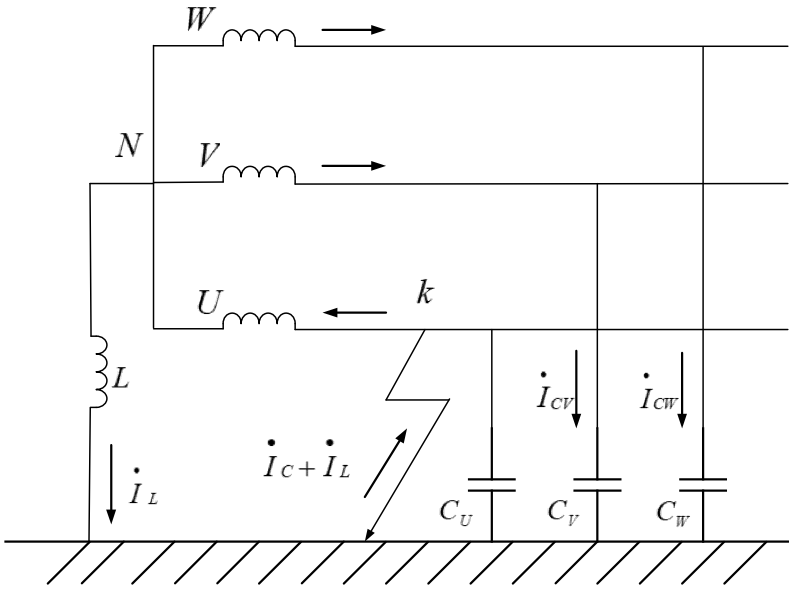


Figure 5. The neutral point through the arc-extinguishing coil grounding system occurs according to the single-phase ground fault diagram.

In the formula, U_P is the grid line voltage (kV), C is the system's single-phase ground capacitance (F) and the unit capacitance of the general overhead line is 5~6 pF/m.

(2) According to the empirical formula, $I_C = (2.7 \sim 3.3) \times 10^{-3} \times U_P l$

In the formula, U_P is the voltage of the grid line (kV), l (km) is the length of the overhead line and the coefficient 2.7 is applicable to a line without overhead ground wire. A coefficient of 3.3 is suitable for lines with overhead ground lines.

Assuming that the length of the overhead line is 15 km, the capacitance currents obtained using the two calculation methods are 0.4489 A and 0.405 A, respectively, and the capacitance current is selected as the average value of 0.427 A. The compensation principle of the arc suppression coil is to make the grounding currents $\dot{I}_L + \dot{I}_C$ offset each other. However, in practical applications, it is found that when $I_L = I_C$, although the grounding current is zero, at this time, $X_L = X_C$, and the system is prone to series resonance overvoltage, which is not conducive to line insulation. When $I_L < I_C$, the grounding current is capacitive, and resonance may occur when the line is cut off or the frequency drops; when $I_L > I_C$, the grounding current is inductive, and the effect of using a zero-sequence current to judge the line fault is better. Therefore, we chose to select the inductance value of the arc suppression coil according to the over-compensation method, and the compensation degree of the arc suppression coil is generally 10%, which can be calculated by the formula $\frac{I_C - \frac{U_N}{\omega L}}{I_C} = 10\%$, and the inductance value is 0.0828 H.

We used ETAP 2023 to build a 13-node distribution network model to simulate and verify the proposed fault location algorithm. The simulation model is shown in Figure 6:

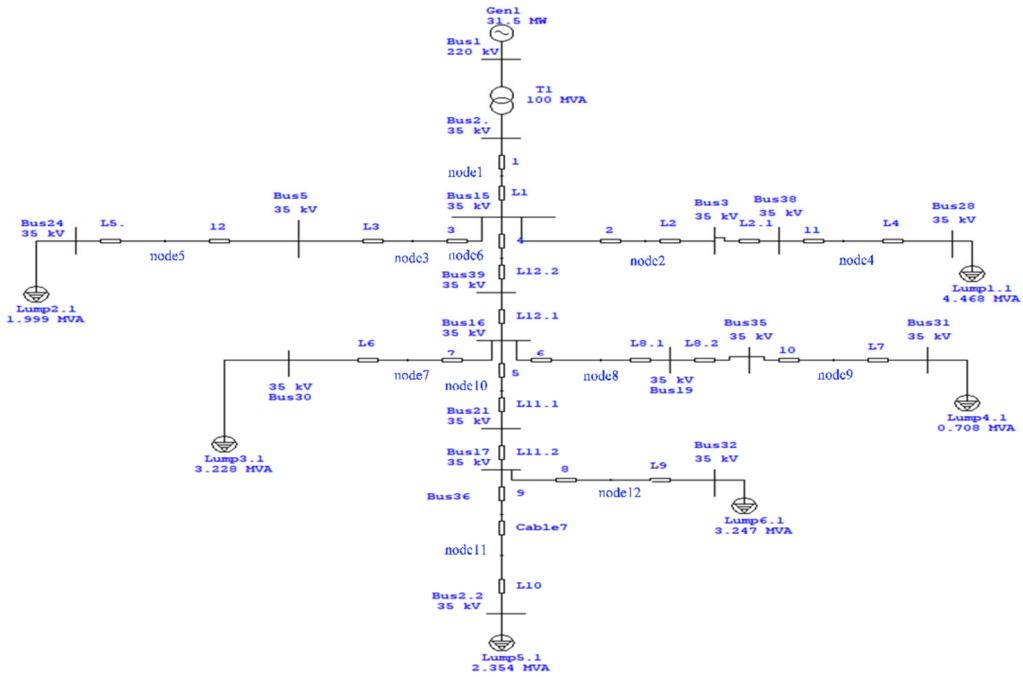


Figure 6. Node distribution network simulation model.

The established distribution network model was set to be powered by a single power supply, and then multiple power supplies could be set according to the simulation requirements. The voltage level of the system power supply was set to 220 kV, the capacity was set to 31.5 MW and 35 kV voltage was obtained through the step-down transformer. The neutral point was grounded through the arc suppression coil, and the grounding inductance value was 0.0828 H.

In the simulation of the matrix algorithm, in order to select the effective fault current node, it was necessary to make a quantitative analysis of the value of the fault current. To accurately identify the correct overcurrent node during simulation, the threshold was set to the minimum short circuit current in a two-phase short circuit network. Simulations revealed that this minimum short circuit current was 7.8 times the normal current level. Consequently, we calculated the fault-to-normal current ratio for all nodes under various fault scenarios. With an allowance for a safety margin, nodes exhibiting a ratio exceeding 7 were deemed to have fault currents passing through them.

The results of section location under a single power supply and single fault could be obtained by simulation, as shown in Table 1.

Table 1. Single-power supply single-fault zone determination results.

Fault Interval	Based on the Fault Section Location of the Current Flow	Judgment Result
Between nodes 8 and 9	Between nodes 8 and 9	True
Nodes 10, 11 and 12 formed a T-region	Nodes 10, 11 and 12 formed a T-region	True
Node 5, feeder end	Node 5, feeder end	True
Between nodes 2 and 4	Between nodes 2 and 4	True
Node 9, feeder end	Node 9, feeder end	True
Between nodes 6 and 7	Between nodes 6 and 7	True

Since nodes 7, 8 and 10 were all exiting the same bus, nodes 6 and 7 or 6 and 8 or 6 and 10 actually refer to the same line between them.

In the case of multiple power supplies, the matrix algorithm based on the current flow expands the judgment of the fault section, and the direction of the fault section expansion is usually upstream of the fault section, while the matrix algorithm based on the voltage quantity usually expands the direction of the fault section downstream of the fault section when judging the fault section. Therefore, when the non-feeder end of the distribution

network fails, two matrix algorithms can be used for joint judgment, and the section intersecting the two judgment results is taken as the final fault section; the judgment results are shown in Table 2.

Table 2. Multi-power source single-fault section determination results.

Fault Interval	Fault Section Location Based on Current Flow	Fault Section Location Based on Voltage	Joint Decision Result	Judgment Result
Node 5, feeder end	Node 1, 6, or node 5, feeder end	Nodes 3 and 5 to the end of the feeders	Node 5, feeder end	True
Nodes 10, 11 and 12 formed a T-region	A T-shaped region consisting of nodes 6 and 7 or 6 and 8 or nodes 10, 11 and 12	Nodes 6 and 7 or 6 and 8 or 6 and 10 or node 7, feeder end	Between nodes 6 and 7	Fault
Between nodes 8 and 9	Between nodes 6 and 7 or 6 and 10 or nodes 8 and 9	Nodes 8 and 9 to the end of the feeders	Between nodes 8 and 9	True
Between nodes 2 and 4	Between nodes 2 and 4 or nodes 1 and 6	Nodes 2 and 4 to the end of the feeders	Between nodes 2 and 4	True
Node 9, feeder end	Nodes 6 and 7 or 6 and 10 or node 9, feeder end	Node 6, 8 or node 9, feeder end	Node 9, feeder end	True
Between nodes 6 and 7	Between nodes 6 and 7 or 6 and 8 or 6 and 10	Node 6 and 7 or 6 and 8 or 6 and 10 or node 7, feeder end	Between nodes 6 and 7	True

Since nodes 7, 8 and 10 were all exiting the same bus, nodes 6 and 7 or 6 and 8 or 6 and 10 actually refer to the same line between them.

From Tables 1 and 2, it can be seen that in the case of a single power supply and single fault, the matrix algorithm based on the current can accurately locate the fault section, whether it is at the end of the feeder, a T-type area or a general line. In the case of a single fault with multiple power sources, the matrix algorithm based on the current cannot accurately locate the fault section. After combining it with the matrix algorithm based on the voltage, the accuracy of section location is greatly improved. Both the feeder end and the general line fault can be accurately located, but when the T-type area fault occurs, the location will deviate.

4. Fault Ranging Algorithm Based on Double-Ended Electrical Quantities

4.1. Fault Ranging Principle Based on Double-Ended Electrical Quantities

The above fault location matrix algorithm can locate the fault between two measurement nodes but cannot give the exact location of the fault point, and the actual 35 kV distribution lines span from several thousand meters to tens of kilometers in length. To enhance the precision of fault location and alleviate the workload of maintenance staff, fault ranging techniques are essential. In this section, a fault location algorithm leveraging dual-end electrical capacitance is introduced. This approach capitalizes on electrical information from both ends to mitigate the impact of transition resistance encountered in single-end location methods [40].

As shown in Figure 7, the fault equivalent diagram of the power line, M and N are the measurement nodes at both ends of the line, the fault points, and the total length of the line. R_{Af}, R_{Bf}, R_{Cf} and R_f are the transition resistance of phases A, B, and C, respectively. When $R_{Af} = 0$, $R_f = K$ (K is an arbitrary constant) and $R_{Bf} = R_{Cf} = \infty$, it means that phase A is grounded through the transition resistance. When $R_f = R_{Cf} = \infty$ and $R_{Af} = R_{Bf} = 0$, it means that an AB two-phase short circuit occurs. The same can be said for other fault types.

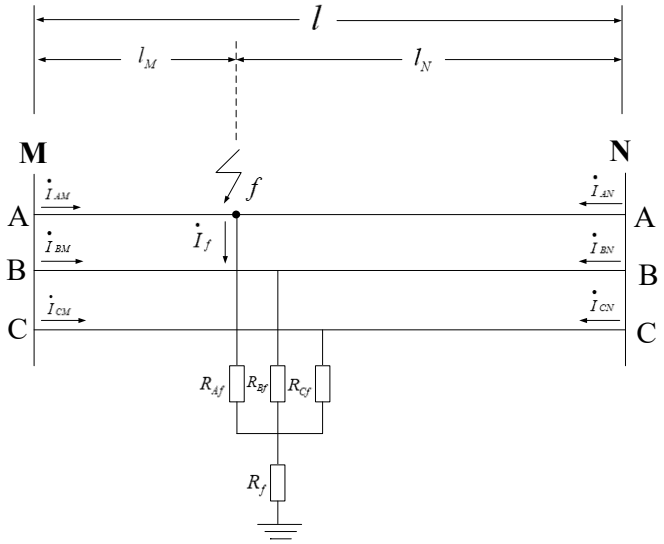


Figure 7. Power line fault equivalence diagram.

Taking single-phase grounding through transition resistance in phase *A* as an example, the fault voltage measured at point *M* is

$$\dot{U}_{AM} = \dot{U}_{AK} + \dot{I}_{1AM} Z_1 l_M + \dot{I}_{2AM} Z_2 l_M + \dot{I}_{0AM} Z_0 l_M \tag{17}$$

In the above formula, $\dot{U}_{AK}$ is the voltage to ground at the fault point of phase A. $\dot{I}_{1AM}$, $\dot{I}_{2AM}$ and $\dot{I}_{0AM}$ are the positive-sequence, negative-sequence and zero-sequence currents of phase A measured at point *M*. Z_1, Z_2 and Z_3 are the line unit's positive-sequence, negative-sequence and zero-sequence impedance. l_M is the distance between the fault point and point *M*.

Since $Z_1 = Z_2$, a unified expression of the *M*-side phase voltage can be obtained by simplifying the process:

$$\dot{U}_M = \dot{U}_K + \left(\dot{I}_M + K3\dot{I}_{0M}\right) Z_1 l_M \tag{18}$$

In the above formula, $K = \frac{Z_0 - Z_1}{3Z_1}$ is the compensation coefficient; l_M is the distance from the fault point to *N*.

From $l_N = l - l_M$, the general formula for the distance l_M from fault point f to point *M* can be obtained as follows:

$$l_M = \left| \frac{\left(\dot{U}_M - \dot{U}_N\right) + \left(\dot{I}_N + K3\dot{I}_{0N}\right) Z_1 l}{\left[\dot{I}_M + \dot{I}_N + K\left(3\dot{I}_{0M} + 3\dot{I}_{0N}\right)\right] Z_1} \right| \tag{19}$$

When an interphase short circuit occurs in the system, the zero-sequence current of the line is 0, which can be obtained as

$$l_M = \left| \frac{\left(\dot{U}_M - \dot{U}_N\right) + \dot{I}_N Z_1 l}{\left(\dot{I}_M + \dot{I}_N\right) Z_1} \right| \tag{20}$$

When a grounding short circuit occurs in the system, the following can be obtained:

$$l_M = \left| \frac{\left(\dot{U}_M - \dot{U}_N\right) + \left[\dot{I}_N + K\left(\dot{I}_{AN} + \dot{I}_{BN} + \dot{I}_{CN}\right)\right] Z_1 l}{\left[\dot{I}_M + \dot{I}_N + K\left(\dot{I}_{AM} + \dot{I}_{BM} + \dot{I}_{CM} + \dot{I}_{AN} + \dot{I}_{BN} + \dot{I}_{CN}\right)\right] Z_1} \right| \tag{21}$$

According to the final ranging formula, the parameters $K = \frac{Z_0 - Z_1}{3Z_1}$, Z_1 and l are all line parameters and are easy to obtain. Other phase voltages and currents on the M and N sides can be obtained by fault recording devices on the M and N sides. This method is simple and fast and does not require the secondary processing of the electrical volume, does not need an additional signal injection device, does not need to calculate the fault point's voltage to ground and does not consider the impact of transition resistance. It has good applicability and practical applications.

4.2. Fault Location Process

The fault location process of this study is summarized as follows, and the fault location flowchart is shown in Figure 8:

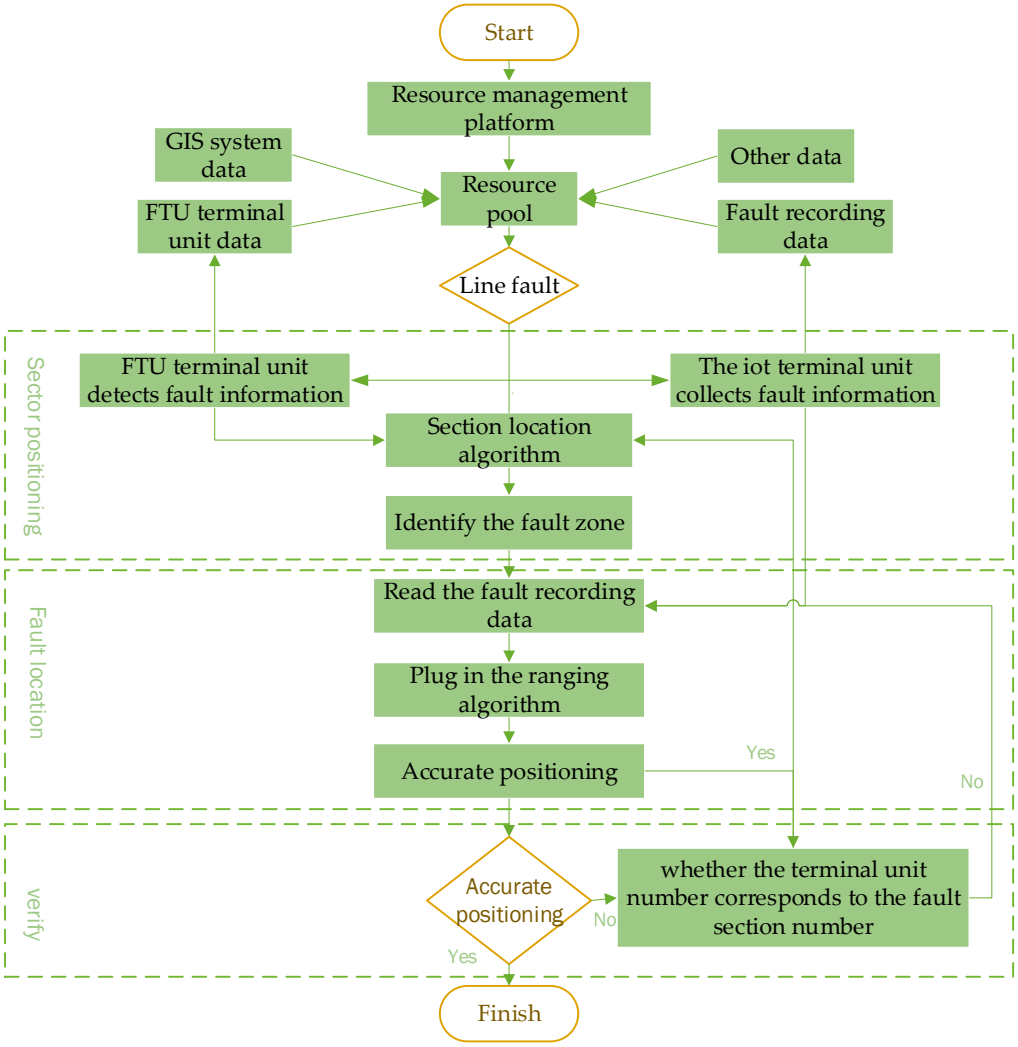


Figure 8. Block diagram of distribution network fault location using multi-source data.

Step 1. After the resource registration, the terminal equipment or systems at the bottom of the distribution network are connected to the cloud computing resource pool together, and then the data resources of the distribution network can be uploaded. The resource management platform can uniformly schedule the data resources according to the business requirements.

Step 2. A line in the distribution network fails.

Step 3. The switch device, voltage transformer, current transformer and Internet of Things terminal device on the line detect the fault information, switch action and upload the fault information.

Step 4. The resource management platform selects the identified fault nodes according to the uploaded overcurrent information, modifies the network description matrix according to the pre-set logical instructions, generates the fault discrimination matrix and then uses the fault criterion to locate the fault section.

Step 5. Based on the uploaded abnormal node voltage information, as in step 4, fault section location is performed.

Step 6. Combining the fault section location information of steps 4 and 5, the section where the location information intersects is selected as the final fault section.

Step 7. The resource management platform preferentially retrieves the fault recording information at both ends of the fault section according to the fault location requirements.

Step 8. The double-ended fault recording information is substituted into the fault ranging algorithm to achieve accurate positioning.

Step 9. Fault ranging verification: Determine whether the ranging result is less than or equal to the length of the section. If correct, output the result directly; if it is not correct, determine whether the terminal unit number corresponds to the fault section number. If it corresponds, return to step 4 and re-locate the fault section. If it does not correspond, return to step 5 and re-extract the recorded data of the corresponding fault section.

Step 10. The end of the fault location: output results.

4.3. Simulation Model Establishment and Verification

The 13-node distribution network simulation model described in Section 3.4 was built in Simulink, and the original model was changed into a two-terminal power supply system. The length of all lines except line L8 was unchanged, and all load parameters were unchanged. Due to the short length and low voltage of the power line, the influence of conductance and susceptance could be ignored. The system frequency was 50 Hz, and the line impedance parameter setting is shown in Table 3.

Table 3. Line impedance parameters.

Parameters	Positive-Sequence Impedance	Zero-Sequence Impedance
R (Ω/km)	0.45	0.7
L (mH/km)	1.1714	3.9065
C/(μF/km)	0.061	0.038

The line between nodes 8 and 9 was taken as the fault line, and the total length of the line was 40 km. B-phase ground short circuit, AB-phase short circuit, BC ground short circuit and three-phase short circuit faults occurred. We set different fault distances and transition resistances of the fault points. The line parameters were extracted, and the unit's positive-sequence impedance = 0.5813 ∠ 39.276° Ω/km, the unit's zero-sequence impedance = 1.4129 ∠ 60.300° Ω/km and the compensation coefficient = 0.5132 ∠ 34.50° were calculated. Through the phasor simulation function of simulink, fault simulation data represented by phasors in a stable state under different fault types, different fault locations and different transition resistances were obtained. Then, the relative error was calculated and the ranging results were analyzed.

4.3.1. Analysis of Ranging Results of Single-Phase Ground Short Circuit

With transition resistances of 0.01 Ω, 20 Ω, 50 Ω, 100 Ω, 200 Ω and 500 Ω, the B-phase ranging results (all as the distance from the M end) are shown in Figure 7.

When the transition resistance was 0.01 Ω, 20 Ω, 50 Ω, 100 Ω and 200 Ω, the relative error of ranging was basically within 0.5%, which met the requirements of the ranging accuracy. When the transition resistance was 500 Ω, due to the large transition resistance, the electrical quantity was weak during the fault, and the relative error was less than 0.7%

when the distance was more than 20 km, which met the accuracy requirements. However, a large error occurred below 15 km, and the measurement error no longer met the ranging requirements. Comparing (a) and (b) in Figure 9, it can be seen that the further away from the measuring end, the more the ranging error decreased; it can be seen that this ranging method has good applicability to a remote single-phase ground short circuit.

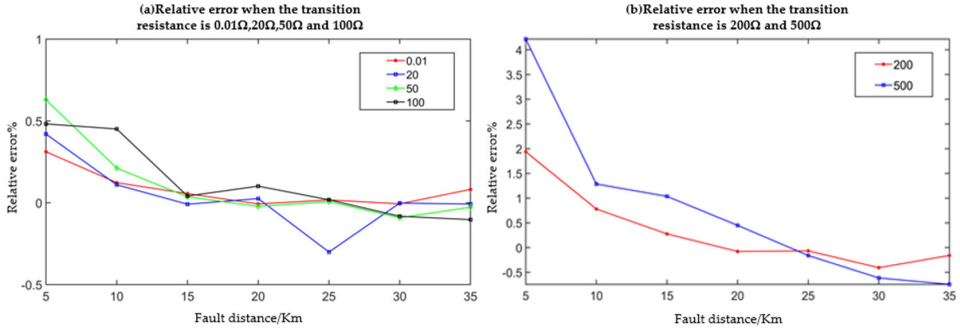


Figure 9. Relative error based on single-phase grounding short circuit.

4.3.2. Analysis of Ranging Results of Two-Phase Ground Short Circuit

From Figure 10, it can be seen that when the fault distance was less than 20 km, the closer the fault point was to the measurement point, the more the relative error would increase, an increase which may have exceeded 0.2% but still met the ranging requirements. When the fault distance was greater than 20 km, the relative error was basically maintained at 0.15%, which met the ranging requirement.

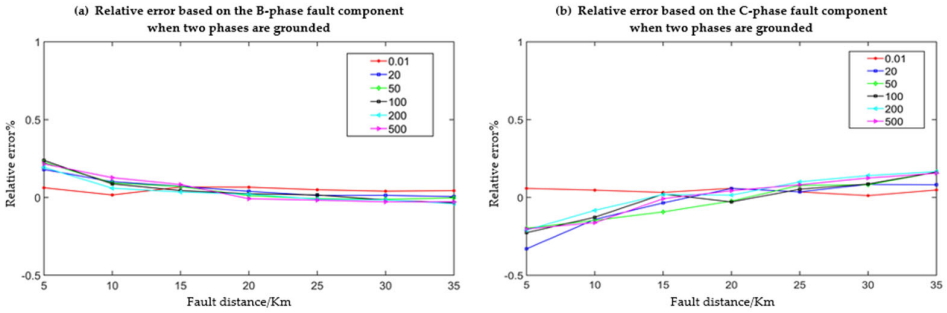


Figure 10. Relative error based on two-phase ground short circuit.

4.3.3. Analysis of Ranging Results of Two-Phase Short Circuit

It can be seen from Figure 11 that in the case of an interphase short circuit, the relative errors calculated based on the fault components of phase A and phase B were both within 0.24%. Even in the case of a near-end fault, the ranging error tended to increase, which far surpassed the ranging requirements. It can be seen that the ranging method has good applicability to an interphase short circuit.

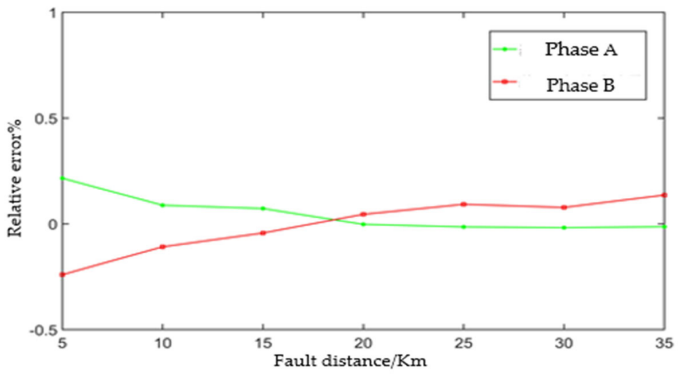


Figure 11. Relative error based on A-and B-phase fault components for two-phase short circuit.

4.3.4. Analysis of Ranging Results of Three-Phase Short Circuit

It can be seen from Figure 12 that in the case of a three-phase short circuit, the relative errors calculated based on the fault components of the A, B and C phases were all within 0.07%, which far surpassed the ranging requirements. When the near end failed, the range error did not increase. It can be seen that the ranging method has good applicability to a three-phase short circuit.

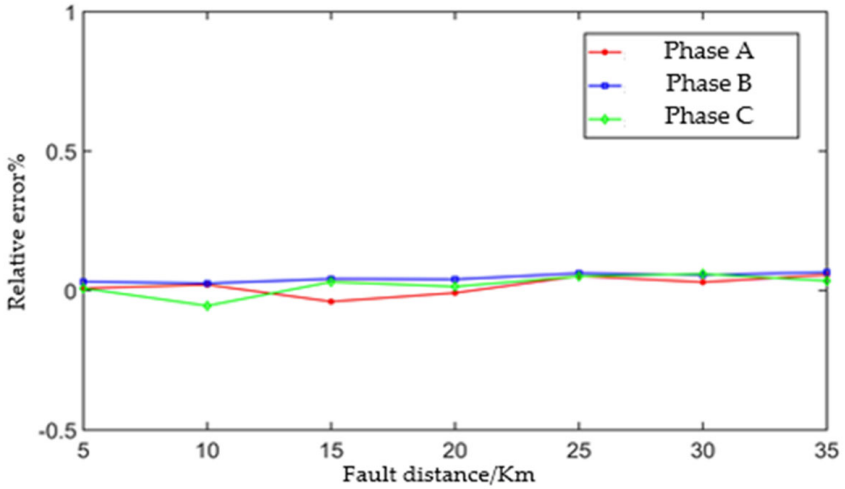


Figure 12. Relative error based on the fault components of phases A, B and C for a three-phase short circuit.

4.3.5. Comparison with Single-Ended Ranging and Directional Relays

In this article, the improved single-ended ranging algorithm proposed in reference [41] is compared and analyzed. The comparative analysis results are as follows.

The following is the comparison of the ranging error in a single-phase grounding short circuit.

From Figures 13–15, it can be seen that when the single-phase ground fault was short-circuited, unlike with the double-ended ranging, the farther the fault point was away from the measurement point, the greater the ranging error was; when the transition resistance was small, the single-ended ranging error was smaller than the double-ended ranging error. As the transition resistance increased, the single-ended ranging error gradually increased and was far greater than the double-ended ranging error.

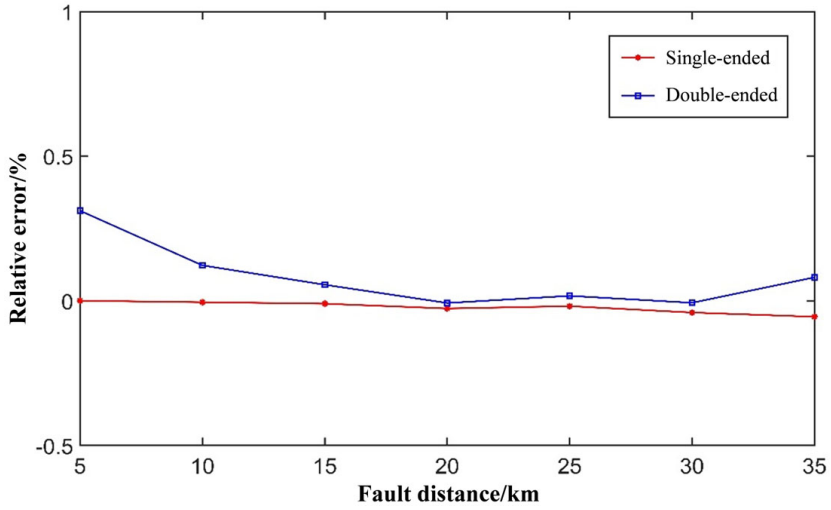


Figure 13. Comparison of ranging error for single-phase ground short circuit with transition resistance of 0.01 Ω.

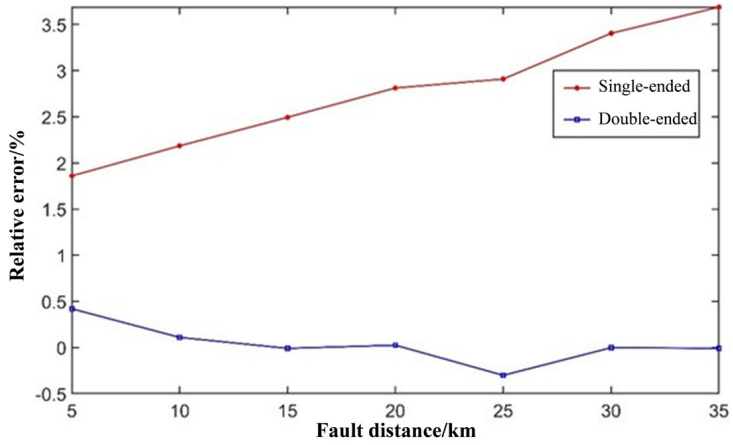


Figure 14. Comparison of ranging error for single-phase ground short circuit with transition resistance of 20 Ω.

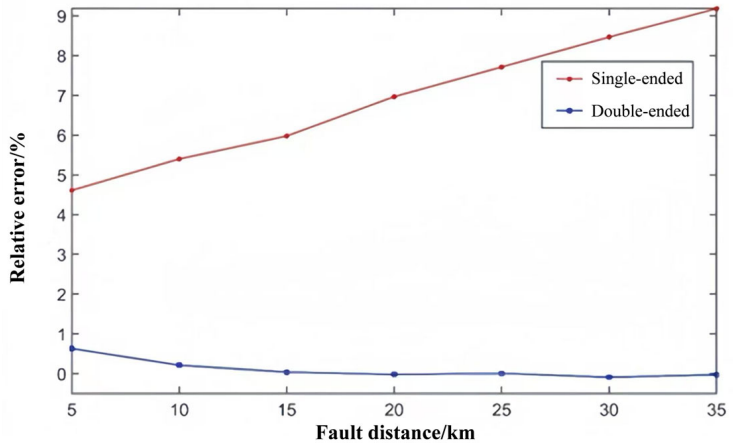


Figure 15. Comparison of ranging error for single-phase ground short circuit with transition resistance of 50 Ω.

From Figures 16–18, it can be seen that when the two-phase grounding short circuit was short, the transition resistance was very small, the ranging error of the two ranging algorithms was not much different and both could achieve accurate fault location; as the transition resistance increased, the single-ended ranging error gradually increased and was far greater than the double-ended ranging error. In contrast, the two-terminal ranging algorithm proposed in this article has more advantages.

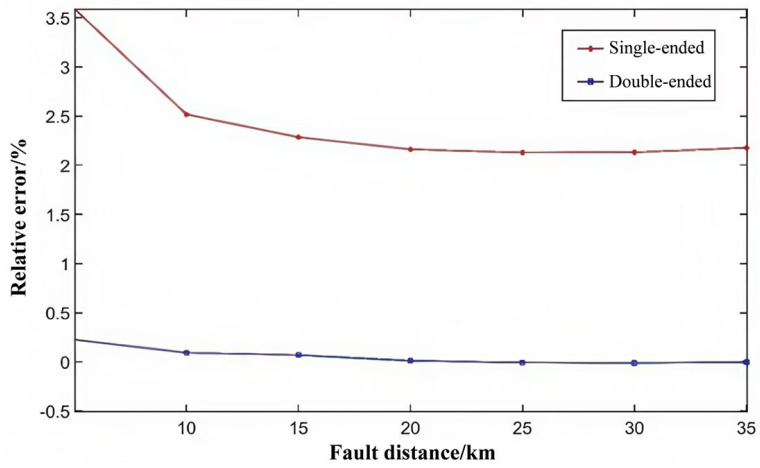


Figure 16. Comparison of ranging error when two phases are short-circuited to ground and the transition resistance is 0.01 Ω.

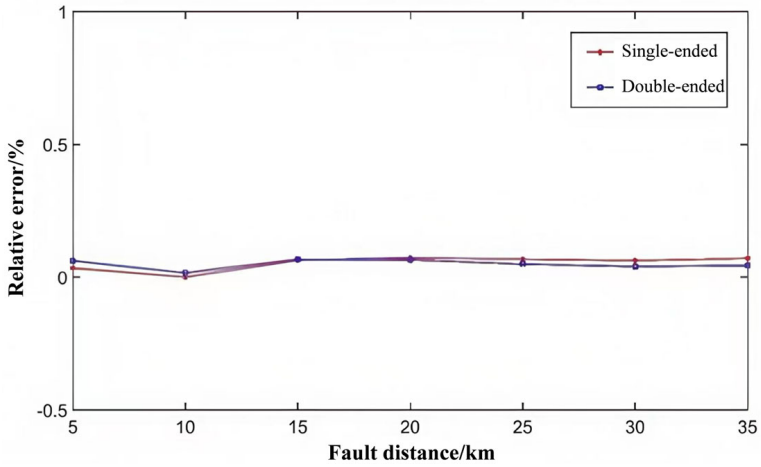


Figure 17. Comparison of ranging error when two phases are short-circuited to ground and the transition resistance is 20 Ω.

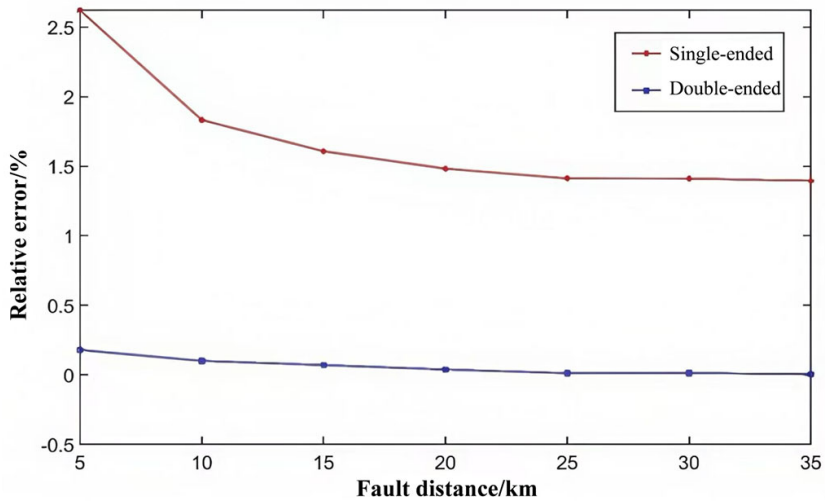


Figure 18. Comparison of ranging error when two phases are short-circuited to ground and the transition resistance is 50 Ω.

In order to visualize the difference between the method in this paper and the directional relay, we performed a simulation comparison analysis. In this study, we used an electric field-coupled voltage sensor with a measurement error range of ±0.5%. This error range was considered in the fault localization algorithm. The simulation analysis showed that the ranging error of the directional relay in a single-phase grounded short circuit was usually large, about 2.1%; in a two-phase short circuit and two-phase grounded short circuit, the errors were 1.8% and 1.2%, respectively; and in a three-phase short circuit, the error was 0.9%. The following is a comparison of the simulation results based on the 13-node distribution network model:

From Figure 19, it can be seen that the method of this paper showed higher accuracy under all fault types; especially in the case of a single-phase grounded short circuit and two-phase short circuit, the error was significantly lower than that of the directional relay method. By analyzing it and comparing it with the directional relay, we found that the method in this paper has obvious advantages in terms of the fault location accuracy. Although the directional relay can determine the direction of the fault, it cannot provide the precise fault location, and its localization error is large. The method proposed in this paper, on the other hand, can effectively improve the accuracy of fault localization, is applicable to a variety of fault types and is not affected by the transition resistance.

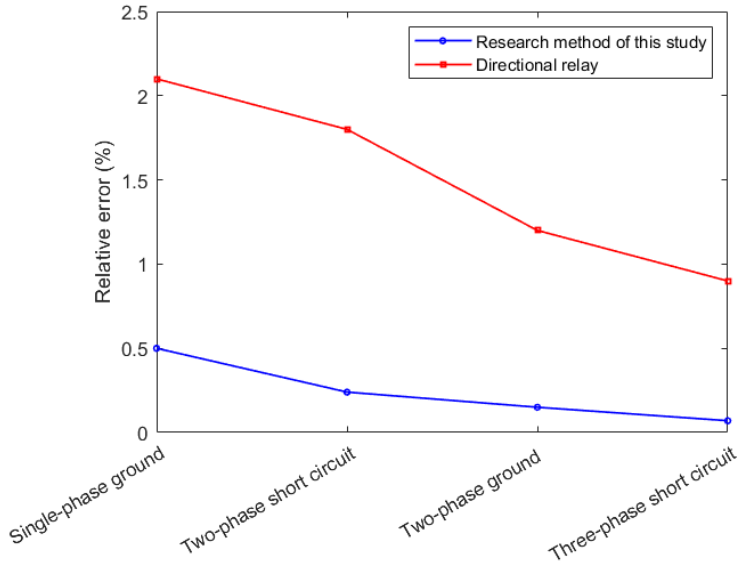


Figure 19. Comparison of location errors with those of directional relays.

5. Discussion

In this study, by fusing multi-source heterogeneous data, a joint matrix algorithm for fault section location and a fault ranging method based on double-ended electrical quantities were proposed to solve the limitations of traditional single-electrical-quantity fault ranging methods. Compared with the existing research, this study showed significant advantages in fault location with multiple power systems and the fault ranging of various fault types. By combining the matrix algorithms of the voltage and current, the positioning problem in multi-power source systems was effectively solved, and the accuracy of fault section positioning was significantly improved. In addition, the double-ended ranging algorithm reduced the influence of transition resistance on the ranging accuracy by using the electrical information at both ends of the fault section and expanded the application range of the ranging method.

By constructing a distribution network data fusion platform based on the resource pool, this study achieved the efficient fusion and processing of multi-source data. In addition, the fault location method proposed in this study can locate the fault quickly and accurately, optimize the traditional fault handling process, reduce the investment of human and material resources and improve the efficiency of fault handling and is of great significance to ensure the stable operation of the social economy. References [3,4] and this study have all tried to improve the fault location accuracy by optimizing the matrix algorithm or introducing new data sources. Although the network relational moment proposed in [4] improves the computational efficiency of the matrix algorithm, it does not address the fault section location problem in multi-power source systems. This study not only optimized the matrix algorithm, but also effectively solved the problem of section location with multiple power systems by combining the matrix algorithms of the voltage and current. Reference [4] used traveling wave information to improve the accuracy of fault location, but it needed more detection devices and had higher requirements for data synchronization. The double-ended ranging algorithm in this study is based on double-ended electrical quantities, without additional detection devices, and has lower requirements for data synchronization and stronger applicability. In comparison with reference [41], it was found that when a single-phase grounding short circuit occurs, the farther the fault point is from the measurement point, the greater the ranging error is, and it is greater than the ranging error of the double-ended ranging method proposed in this article. However, when the transition resistance is relatively small, the single-ended ranging

error is smaller than the double-ended ranging error. When a two-phase ground short circuit occurs, the single-ended ranging error increases with an increase in the transition resistance, and the ranging accuracy is much lower than the double-ended ranging error.

Although this study has made breakthroughs in many aspects, there are still some shortcomings. Firstly, the ranging error of the double-ended ranging algorithm is relatively large when a single-phase ground short circuit occurs, and the near-end ranging error especially is more significant. This shows that the accuracy of the algorithm still needs to be improved under certain fault types. We considered using the method of measuring the remote distance to reduce the ranging error, but it was found that the error was not reduced. Through comparative analysis, it was found that along the direction of the line's power flow, the farther away from the measurement point, the smaller the ranging error. The farther away from the measurement point, the greater the ranging error.

The fault location method for distribution networks based on multi-source information fusion proposed in this study has made significant progress in solving the limitations of traditional single-electrical-fault location methods. Using the joint matrix algorithm and the double-ended ranging algorithm, this study not only improved the accuracy of fault section location, but also enhanced the applicability of the ranging method under various fault types and transition resistance conditions. However, there are still some shortcomings in the research, such as the large ranging error when a single-phase grounding short circuit occurs, and the applicability in more complex fault scenarios has not been fully verified. Future research will focus on further optimizing the algorithm to improve its performance and universality in various complex scenarios.

6. Conclusions

The diverse structure of modern distribution networks brings difficulties to accurate fault location. The traditional method of fault location using a single electrical quantity shows many limitations in today's increasingly complex distribution network structure. With the development of the automatic technology of distribution networks, it is not difficult to obtain multi-source fault data, and the key to fault location is hidden in rich multi-source fault data. Therefore, based on the electric field coupling voltage sensing and fusion of multi-source data, this article proposes a joint matrix algorithm for fault section location and a fault ranging method based on a double-ended electrical quantity.

The main work of this article is as follows:

(1) The measurement principle of an electric field coupling voltage sensor is introduced, and the fault location method for distribution networks was studied based on this non-contact sensor. In order to make full use of data from different sources and improve the accuracy of fault location, the design concept and basic architecture of a distribution network data fusion platform based on the resource pool are proposed. The process of the multi-source data fault location flow is introduced in detail.

(2) By analyzing the principle of a traditional matrix algorithm based on a directed graph, this paper proposes an improved matrix algorithm based on a directed graph, which solves the problem of the inaccurate location of the traditional matrix algorithm in a multiple-power-supply system. Based on the phenomenon that the matrix algorithm based on the current may cause the expansion of fault section location, the limitations of the matrix algorithm based on the current for s location in the case of a single fault with multiple power sources were addressed by introducing the voltage quantity information. The improved matrix algorithm performs well in dealing with complex network structures (e.g., T-area and feeder end faults) and can effectively reduce the expansion of the location range and improve the section location accuracy.

(3) After fault section location, a fault ranging algorithm based on double-ended electrical quantities was proposed. A simulation model was built, and the ranging results under different fault conditions were simulated and analyzed. Compared with the single-ended ranging algorithm, the ranging error of this method is significantly smaller, which proves that the method is applicable to a wide range of fault types (including single-phase ground, two-phase short circuit, two-phase grounded short circuit and three-phase short circuit faults) and that the ranging accuracy is high, independent of the fault location and transition resistance, which makes the method well suited for use.

(4) Although the resource management system proposed in this article has a corresponding software platform, it is still difficult to realize the access to and integration of distribution network data. In the future, the corresponding platform can firstly be applied to the regional distribution network for testing, and after the test results are good, accessing more and more extensive distribution network terminals can be considered. In addition, the matrix algorithm for fault segment location proposed in this article adopted only one distribution network model in the simulation verification and does not consider the impact of distributed power access on the fault location. In our next research, we will focus on fault location for the distribution network after accessing the distributed power supply.

Author Contributions: Conceptualization, B.L. and L.L.; methodology, L.T. and Z.G.; software, B.L. and L.T.; validation, L.T. and Z.G.; formal analysis, B.L.; investigation, Z.G.; resources, Z.W.; data curation, B.L and L.T.; writing—original draft preparation, L.L.; writing—review and editing, L.T., Z.G., L.L. and Z.W.; visualization, L.T.; supervision, B.L.; project administration, B.L.; funding acquisition, Z.W. All authors have read and agreed to the published version of the manuscript.

Funding: This research was supported by Yunnan Power Grid Co., Ltd., Electric Power Science Research Institute, 0562002024030301JL00007.

Data Availability Statement: Data are contained within the article.

Conflicts of Interest: Authors Bo Li, Lijun Tang and Zhiming Gu were employed by the company Yunnan Power Grid Co., Ltd. The remaining authors declare that the research was conducted in the absence of any commercial or financial relationships that could be construed as a potential conflict of interest.

References

1. Li, Z. Fault Section Location Method Based on Wide Area Measurement. *Guangdong Electr. Power* **2017**, *30*, 68–73.
2. Liu, J.; Ni, J.; Du, Y. Unified Matrix Algorithm for Fault Section Judgment and Isolation of Distribution Network. *Autom. Electr. Power Syst.* **1999**, *01*, 31–33.
3. Huang, J.; Yang, G. Improved Matrix Algorithm for Fault Location in Distribution Networks. *Electr. Power Syst. Res.* **2014**, *42*, 41–45.
4. Zhang, W.; Li, J.; Wang, X. Improved Matrix Algorithm for Fault Location in Distribution Networks Based on Multi-terminal Traveling Wave Information. *Hydropower Energy Sci.* **2021**, *39*, 194–197+170.
5. Wang, Y.; Jia, Y. Improved Matrix Algorithm for Fault Location of Distributed Power Distribution Network. *Comput. Simul.* **2018**, *35*, 58–64.
6. Deng, F. Distribution Network Fault Location Method Based on Directed Topology-time Delay and Fault Tolerance Mechanism. *Electr. Autom.* **2019**, *41*, 73–77.
7. Gao, Y. *Study on Fault Location of Distribution Network Based on Improved Matrix Algorithm*; Shenyang Institute of Engineering: Shenyang, China, 2020.
8. Liang, Z.; Yang, M. A Distribution Network Fault Location Method Based on Graph Theory and Improved Matrix Algorithm. *Guangxi Electr. Power* **2021**, *44*, 69–76.
9. Liang, Y.; Tian, S.; Liu, M. Fault section location of multi-source distribution network based on phasor correction. *Power Syst. Prot. Control* **2023**, *51*, 33–42.

10. Zeng, H.; Yang, C. Fault Location Matrix Algorithm for Distribution Network Based on Voltage Amplitude Correction. *Electr. Power Sci. Eng.* **2020**, *36*, 41–46.
11. Hou, S. Distribution Network Fault Section Location Method Based on Wavelet AlexNet Network. *Electr. Meas. Instrum.* **2022**, *59*, 46–57.
12. Zhang, L. Fault Location of Distribution Network Based on Adaptive Genetic Particle Swarm Optimization. *J. Chongqing Univ. Technol. (Nat. Sci.)* **2021**, *35*, 160–168.
13. Wu, J.; Xue, Y.; Shan, C.; Tan, Q. Research on Fault Location of Distribution Network Based on Improved Artificial Fish School Optimization Algorithm. *Proc. CSEE* **2023**, *38*, 40–47.
14. Xing, X.; Shi, F.; Zhang, H.; Sun, B.; Shi, Z. Adaptive Fault Section Location Method for Active Distribution Network Based on Synchronized Phasor. *Trans. China Electrotech. Soc.* **2020**, *35*, 4920–4930.
15. Tang, J. Review on Automatic Fault Location Technology of Distribution Network. *Electr. Power Autom. Equip.* **2013**, *33*, 7–13.
16. Li, B.; Zhang, X.; He, J.; Sun, Q.; Li, Y.; Zhou, B.; Xie, Z. Fault Distance Measurement Method for Double-Loop Cross-Line Grounding Fault of DC Pole Based on High Frequency Measurement Impedance Amplitude and Phase Characteristics. *Power Syst. Technol.* **2022**, *46*, 4645–4656.
17. Shu, H.; Liu, X.; Tian, X. Single-ended fault location for hybrid feeders based on characteristic distribution of traveling wave along a line. *IEEE Trans. Power Deliv.* **2020**, *15*, 71–76. [CrossRef]
18. Druml, G.; Raunig, C.; Schegner, P.; Fickert, L. Earth Fault Localization with the Help of the Fast-pulse-detection-method Using the New High-Power-Current-Injection (HPCI). In Proceedings of the 2012 Electric Power Quality and Supply Reliability, Tartu, Estonia, 11–13 June 2012.
19. Liang, D.; Xu, B.; Xie, W.; Liu, Y. Fault Distance Measurement Method for Cable Based on Wavelet Pulse Correlation. *Proc. CSEE* **2020**, *40*, 8050–8057+8241.
20. Xia, J. A New Algorithm for Two-terminal Fault Location Based on Longitudinal Impedance. *Electr. Power Autom. Equip.* **2015**, *35*, 133–139.
21. Gao, H.; Chen, X.; Liu, H.; Li, C.; Feng, Y. Fault Distance Measurement Algorithm Based on Improved Parameter Detection Method for Dual-End Asynchronous Data. *Electr. Power Autom. Equip.* **2014**, *34*, 27–32.
22. Zhou, W. A New Fault Distance Measurement Method Based on Parameter Unknown Asynchronous. *Ind. Control. Comput.* **2014**, *27*, 151–152.
23. Lin, J.; Chen, R.; Li, Y.; Chen, W. Fault Location Method for Distribution Network Based on Parameter Identification. *South. Power Syst. Technol.* **2019**, *13*, 80–87.
24. Zhao, Y.; Xiao, S.; Jiao, S.; Liu, W. Data synchronization and fault location of line recording based on least square method. *Electr. Power Eng. Technol.* **2020**, *39*, 78–84.
25. Tian, B.; Fang, Q.; Li, Z.; Li, Z.; Liu, B. Traveling Wave Distance Measurement Algorithm for Multi-Circuit Transmission Lines Based on Wave Velocity Correction. *High Volt. Appar.* **2019**, *55*, 184–189.
26. Ding, J.; Wang, X.; Zheng, Y.; Li, L. Improved Single-End Traveling Wave Fault Distance Measurement Method Based on Midpoint Current Detection. *High Volt. Technol.* **2020**, *46*, 1814–1822.
27. Li, Z.; Wu, L.; Tian, B.; Li, Z. Research on Single-End Traveling Wave Distance Measurement Algorithm Based on Asynchronous Double-End Data Corrected Wave Velocity. *Electr. Power Syst. Res.* **2017**, *45*, 16–22.
28. Liu, L.; Deng, M.; Zhang, M.; Zhou, F. A New Method for Fault Distance Measurement in Distribution Network Compensating High Frequency Capacitive Effect of Distribution Transformer. *J. Chang. Univ. (Nat. Sci.)* **2021**, *35*, 6–12.
29. Li, L.; Sun, T.; Zeng, S.; Wang, L.; Liang, J. Fault Location Method for Distribution Network Based on Multi-Terminal Traveling Wave Time Difference. *Electr. Power Syst. Res.* **2022**, *50*, 140–147.
30. Lee, J.; Kao, H.; Yang, S. Service Innovation and Smart Analytics for Industry 4.0 and Big Data Environment. *Procedia CIRP* **2014**, *16*, 3–8. [CrossRef]
31. Liu, X.; Huang, C. Application of Ant Colony Algorithm to Fault Location of Ultra-high Voltage Transmission Lines. *J. Electr. Power Syst. Autom.* **2012**, *24*, 132–137.
32. Gao, B.; Zhang, C.; Li, H.; Tian, Y.; Yang, J. Research on Fault Distance Measurement Model of Transmission Line Based on Improved Ant Colony Algorithm. *Autom. Instrum.* **2022**, *43*, 61–64.
33. Zheng, C.; Zhou, H.; Zheng, D.; Lin, Z.; Zhang, X. Research on Fault Location Method of Active Distribution Network Based on Improved Multi-Universe Optimization Algorithm. *Electr. Power Syst. Res.* **2023**, *51*, 169–179.
34. Zhang, L. *Research on Power Grid Fault Diagnosis Based on Multi-Data Source Information Fusion*; Northeastern University: Shenyang, China, 2013.
35. Li, J.; Ding, H.; Li, L. Research and Application of Decentralized DTU Terminal Communication Technology. *Hubei Electr. Power* **2021**, *45*, 98–102.
36. Jin, P. *Research on Distribution Network Fault Location*; Tianjin University of Technology: Tianjin, China, 2015.
37. Jiang, X.; Xiong, X.; Wu, Y.; Tang, J. Improved Matrix Algorithm and Its Application in Distribution Network Fault Location. *Power Grid Technol.* **2004**, *19*, 60–63.

38. Xie, Y. Research on Distribution Network Fault Location Based on Improved Matrix Algorithm. *J. Electr. Power* **2011**, *26*, 199–201.
39. Hu, G.; Cao, K.; Meng, Y.; Zhang, Y. Research and Analysis of Fault Location Method for Low-voltage Distribution NetworkBased on the Characteristic of Full Current Direction. *Electr. Power Inf. Commun. Technol.* **2024**, *22*, 83–90.
40. Zhang, J.; Zhou, P.; Chen, H. Simulation of Single-phase Ground Fault Location Based on Improved Impedance Method. *Electr. Meas. Instrum.* **2018**, *55*, 84–87.
41. Niu, T. *Research on Single-Phase Grounding Fault Location of Distribution Network Based on Multi-Source Information*; University of Jinan: Jinan, China, 2021.

Disclaimer/Publisher's Note: The statements, opinions and data contained in all publications are solely those of the individual author(s) and contributor(s) and not of MDPI and/or the editor(s). MDPI and/or the editor(s) disclaim responsibility for any injury to people or property resulting from any ideas, methods, instructions or products referred to in the content.